Available online at www.sciencedirect.com

ScienceDirect

journal homepage: www.elsevier.com/locate/he

Effect of low B addition on Al-Zn alloy's hydrogen production performance

Mehmet Fatih Kaya [a], *Osman Kahveci* [b,*], *Harun Erol* [c], *Abdullah Akkaya* [d]

[a] *Erciyes University, Engineering Faculty, Energy Systems Engineering Department, Heat Engineering Division, 38039, Kayseri, Turkey*

[b] *Erciyes University, Faculty of Science, Physics Department, 38039, Kayseri, Turkey*

[c] *Çankırı Karatekin University, Faculty of Science, Physics Department, 18100, Çankırı, Turkey*

[d] *Kırşehir Ahi Evran University, Mucur Vocational School, Chemistry and Chemical Process Technologies Department, 40500, Kırşehir, Turkey*

HIGHLIGHTS

- Low B addition effect to the Al2Zn alloy's hydrogen production is investigated.
- In Al2Zn0.5B alloy, 83% higher hydrogen generation performance is obtained.
- Oxide film is more fragile and porous by the help of AlB_2 phase.
- By low B addition, activation energy is lowered from 26.717 to 23.526 kJ mol^{-1}.
- By addition of 0.5wt.%B to Al2Zn, 1.83 times higher G_{H2} value is obtained.

GRAPHICAL ABSTRACT

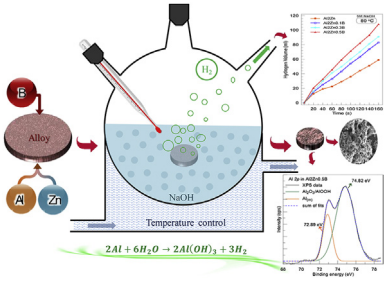

ARTICLE INFO

Article history:
Received 11 September 2020
Received in revised form
15 December 2020
Accepted 10 February 2021
Available online 9 March 2021

Keywords:
Hydrogen production
Al-Zn Alloy
Boron

ABSTRACT

Aluminium hydrolysis is a promising method for hydrogen generation due to its instant hydrogen production, simplicity, controllability, and safety properties. Moreover, Al is very common, recyclable, lightweight material and it has no degradation problem to supply hydrogen in energy conversion devices. Hydrogen produced by Al can be easily adapted to fuel cells to convert energy into higher efficiency. In this study, the effect of low B additions (0.1, 0.3, and 0.5 wt.%) to the Al-2wt.%Zn alloy's hydrogen generation performance is investigated. Different temperatures (25, 50, and 80 °C) and different concentrations of NaOH (1, 3, and 5 M) are studied to observe their effects on the hydrogen production and corrosion rate. At 80 °C and 5 M NaOH concentration, in Al-2wt.%Zn-0.5wt.%B alloy, around 83% higher hydrogen generation performance is obtained than Al-2wt.% Zn alloy. The hydrolysis reaction kinetics are investigated with the Arrhenius equation and by low B addition, activation energy of the Al-2wt.%Zn and Al-2wt.%Zn-0.5 wt.%B alloys are decreased from 26.717 kJ mol^{-1} to 23.526 kJ mol^{-1}.

* *Corresponding author.*
E-mail address: kahveci@erciyes.edu.tr (O. Kahveci).

https://doi.org/10.1016/j.ijhydene.2021.02.086

Aluminium boride
Alkaline media

Introduction

Increasing world population, technological and economic developments are caused the high energy consumption, environmental problems and depletion of the fossil energy sources. This situation makes renewable energy production vitally important. Among the other fuels, hydrogen is seen as the best alternative to other fuels because of its high energy density and environmentally friendly properties [1]. However, as an energy carrier, hydrogen should be produced from water and hydrocarbons [2] by biological [3], water electrolysis and splitting [4,5], steam and partial oxidation [6,7] and biomass [8] methods. Recently, reactive metals, such as Al, Zn, Mg, etc. is extensively used to produce hydrogen by several chemical reactions [2]. Among these metals, Al is seen as the most promising candidate to produce higher hydrogen volumes [9]. Because, Al has low cost, high energy density (29 MJ kg^{-1}), fully recyclable and lightweight (2700 kg m^{-3} density value) properties. Due to its lightweight specification, it is possible to use this metal in portable systems for energy conversion applications [10,11]. The corrosion reactions of Al have minimum environmental impact without CO_2 products. Through the Al-Water reactions, aluminium oxide (Al_2O_3) and aluminium hydroxide ($Al(OH)_3$) are formed. These products are very beneficial for the water treatment studies. Moreover, it is possible to obtain Al from Al_2O_3 compounds by the Hall–Heroult process. Moreover, wide spreading of electrical cars brings some range problems due to the capacity problems of commonly used Li-ion batteries. Fuel cells can be a good alternative for this range extension studies and it is possible to drive a fuel cell powered car by 400 km with only 4 kg of aluminium [12]. Al and its alloys also can be used as battery electrode with their high potential and low corrosion properties. Recently, pure aluminium or doped aluminium alloys have adequate properties to supply storage needs. Furthermore, waste aluminium which are not possible to recycle from secondary aluminium product also can be used as low-cost hydrogen generation metal [2]. For example Ho et al. [13] used waste aluminium cans in low alkaline media to produce hydrogen gas with Ni/Bi additives. They concluded that, this method is comparable with pure aluminium powders' hydrogen production performance for sustainable hydrogen production. They observed that, lower particle size has higher hydrogen production rates due to its closed contact with alkaline media. Chemical energy stored in Al metal can react with water to obtain hydrogen gas. However, Al is tended to oxidize with water-Al reactions, and it is caused oxide film on the surface of Al metals which has adverse effect on the hydrogen production performance. Thus, alkaline media, such as NaOH or KOH aqueous solutions [14–16] or ball milling process [17–19] can be used to lowering oxide film's negative effect on the hydrogen production performance. In aluminium hydrogen generation with the assistance of alkali occurs by following reaction steps:

$$2Al + 6H_2O + 2NaOH \rightarrow 2NaAl(OH)_4 + 3H_2 \quad (1)$$

$$NaAl(OH)_4 \rightarrow NaOH + Al(OH)_3 \quad (2)$$

$$2Al + 6H_2O \rightarrow 2Al(OH)_3 + 3H_2 \quad (3)$$

In the step (1) NaOH is consumed to regenerate $NaAl(OH)_4$ composition in step (2). Thus, if reactions is controlled very properly only water is consumed as seen in net reaction at step (3). These reactions testify that aluminium is a compact source of hydrogen and it can be used extensively like hydrogen storage device. Thus, several hydrogen generation or supply devices are develop based on these reactions [20–26].

In these reactions, some inorganic additives are used to observe effect of Al-metal hydrogen production performance such as, $AlMoO_3$, $AlBi_2O_3$, and AlCuO and some inert composites like Al-MgO and Al-Al_2O_3 [27]. Furthermore, active metals are another option to obtain higher hydrogen production rates. For example, Li [28], Ce [29] and Ca [30] are used to improve Aluminium hydrolysis reaction performance for different applications. Moreover, to improve Al activation, low melting point metals like Ga, In, Sn, Zn, Bi and Mg are used as the alloying metals [1,31,32]. In these studies, Al powder is mechanically alloyed with these metals to observe difference of hydrogen production performance with un-milled Al powder. For example, Wang et al. [33]. doped Ga, In and Sn to Al metals to observe alloys' hydrogen production performance. They concluded that lower particle size of alloys has higher hydrogen production amount and 30% less activation energy than bigger particle size alloy metals. Preez et al. [34] investigated the aluminum-tin-indium composites' hydrogen production performance in pure water. They observed some AlSn phases in ternary composites and more than 95% hydrogen yield is obtained. In another study, Wang et al. [1] investigated hydrogen generation performance of binary, ternary and quaternary alloys of Al with Ga, In and Sn elements. They obtained higher performance in ternary and quaternary alloys. Efficiency of the hydrogen production is reached around 100% in quaternary alloys (3%Ga, 3%In, 5%Sn and Al).

However, besides alloying of aluminium, there are many other factors that affect the hydrogen production performance. For example, temperature, alkali concentration, morphology, metal amount, concentration of metal ions may affect the performance of the metallic hydrogen production. Thus, alloying of aluminium needs parametric study to optimize temperature, alkaline concentration and metallic properties and pre-treatment of reactants [16]. For example, Du et al. [35] investigated the effect of different Mg content (from 2wt.% to 7wt.%) doping to Al-Mg-Ga-In-Sn alloy by preparing casting and melting methods. They investigated that Mg

content and temperature of the water is crucial parameters for the reaction speed of hydrogen generation. Park et al. [36] investigated the corrosion ratio has the highest value in Al-Zn which is very crucial parameter for the hydrogen generation reactions. Due to the Zn's low melting point it reacts very well in alkaline media when alloying with Al. Zn may also increase the hydrogen production rate and yield with enhancing pitting corrosion amount of Al alloys [37]. However, according to author's knowledge, there is not any study that investigates the effect of low B doping on the Al-Zn alloy's hydrogen generation performance as ternary alloy.

Thus, in the present work, low B doping (0.1, 0.3 and 0.5wt.%) to the Al-wt.%2Zn is studied to investigate hydrogen performance effect in alkaline media. Different temperature and solution concentrations are used to observe different parameter's effect on low B added Al-wt.%2Zn alloys' hydrogen generation performance. Samples are physically characterized by Field Emission-Scanning Electron Microscopy (FE-SEM), FE-SEM- Energy-Dispersive X-ray Spectroscopy (FE-SEM-EDX) and X-Ray Photo Spectroscopy (XPS) analysis. Hydrogen generation amounts are measured by time and activations energies of the samples are calculated to observe their reaction kinetics.

Materials and methods

Preparation of samples

To prepare hydrogen production alloy samples, Al (99.99% purity) and Zn elements (99.99% purity) and B metallic element (99.5% purity) are used as alloying elements for casting process. Firstly, Al-2wt.%Zn (Al2Zn) master alloy casting process is performed. To prepare master alloy, Al element is placed in a quartz tube and heated to 700 ± 10 °C for 2 min in an induction furnace. Then, Zn element is added to molten Al in the same temperature for 3 min to obtain homogeneous mixture.

Secondly, B addition is performed to Al2Zn master alloy to obtain Al2Zn-0.1wt.%B (Al2Zn0.1B), Al2Zn-0.3wt.%B (Al2Zn0.3B) and Al2Zn-0.5wt.%B (Al2Zn0.5B), respectively. A graphite mold (10 mm diameter and 50 mm length) is used for mechanical casting, this mold is preheated to 700 °C before casting process. Then, alloys are mechanically casted in this mold and remained for cooling in room temperature. For B added alloys, B elements are added to the process by increasing temperature to 1000 ± 50 °C in melting step. 10 mm diameter and 50 mm length cylindrical Al2Zn binary and Al2Zn0.1B, Al2Zn0.3B, Al2Zn0.5B ternary alloys are obtained, successfully.

Afterwards, metallographic process is performed to cylindrical samples. Firstly, samples are cut to 2 ± 0.01 mm thickness with cutting device (Struers Minitom). Secondly, samples are polished mechanically by the help of waterproof silicon carbide (SiC) papers with 600, 800, 1200, 2400, 4000 grids.

Characterization of alloy samples

After alkaline media reactions, all samples are cleaned by extra pure water (Milli-Q®) and dried in nitrogen vacuum atmosphere at 50 °C. To observe surface morphologies of the samples, FE-SEM (Zeiss Gemini 500) and FE-SEM-EDX (EDAX Inc.) analysis are performed.

X-ray photoelectron spectroscopy (XPS) analysis (Specs-Flex XPS) are performed to characterize the morphology and surface composition of alkaline media immersed different alloys. XPS studies are performed on Al2Zn, Al2Zn0.1B, Al2Zn0.3B and Al2Zn0.5B alloys. These samples are dipped in 5 M NaOH at 80 °C for a 160 s, and after rinsed and dried for XPS measurements.

Hydrogen generation measurements of alloys

In Fig. 1, experimental setup of hydrogen production reactor can be seen. To measure hydrogen production, three necked round bottomed flask (500 ml) and different concentration of NaOH aqueous solutions are used as hydrogen production reactor.

Temperature is controlled by a heating cooling system (Polyscience Recirculating Chiller) and changed between 25 and 80 °C to obtain constant temperature. In temperature depended studies, 5 M NaOH aqueous solution is used and hydrogen production amount is measured. For concentration depended studies, solution (1, 3 and 5 M NaOH) temperature is set to 80 °C to observe effect of concentration to Al alloys' hydrogen production performance. All hydrogen gas generation measurements are recorded during 160 s. Samples which are for oxide film examinations are only cleaned by pure water without ultrasonic cleaning. Produced hydrogen gas is cleaned with washing bath (in 25 °C pure water) and accumulated by accumulation tube. To calculate corrosion rate of the samples, weight of the samples is measured before and after 160 s immersion time. In addition, oxide film on the surface of the samples are washed by 2% CrO_3 and 5% H_3PO_4, respectively [38–42].

Results and discussions

Hydrogen generation performance of alloys

Al2Zn binary alloy and different B added Al2Zn ternary alloys are tested to investigate their hydrogen generation performance. All alloying samples are prepared in 2 ± 0.01 mm thickness and 10 ± 0.01 mm diameter with 2.20 ± 0.04 cm^2 active surface area. Hydrogen production experiments are conducted in different concentration (1–5 M) of NaOH aqueous solution and different temperatures between 25 and 80 °C. In Fig. 2a, b and c, hydrogen generation amount of different Al2Zn alloys can be seen in 5 M and 25, 50 and 80 °C, respectively. Hydrogen gas evaluation rate ($G_{H2)}$ of different samples are listed in Table 1.

As seen in Fig. 2a, b and c, increasing temperature from 25 °C to 80 °C G_{H2} value is enhanced, significantly. At the same time, addition of B to Al2Zn alloy is increased hydrogen generation amount and G_{H2} for all samples. It can be seen in Fig. 2a, b, and c, in 25 °C, 50 °C and 80 °C maximum hydrogen production amounts are obtained in Al2Zn0.5B alloy as 4.5 ml, 42 ml and 108 ml, respectively. In 80 °C and 5 M NaOH aqueous solution, while hydrogen production amount is 59 ml in Al2Zn

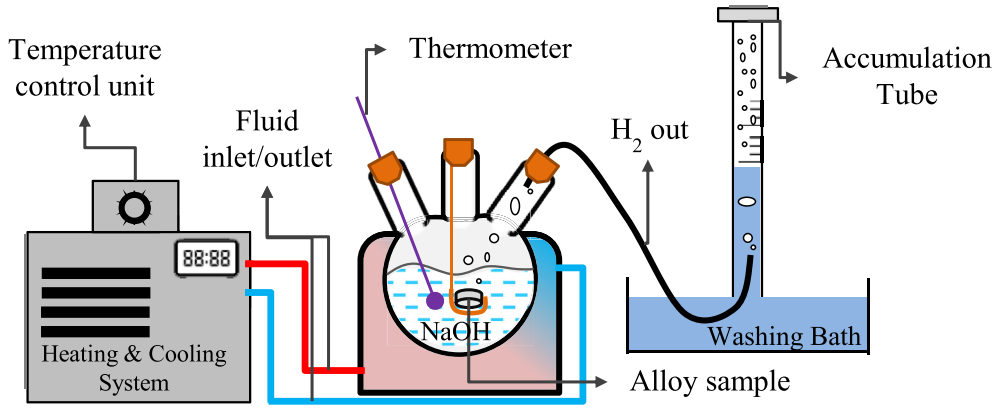

Fig. 1 – Hydrogen production experimental setup.

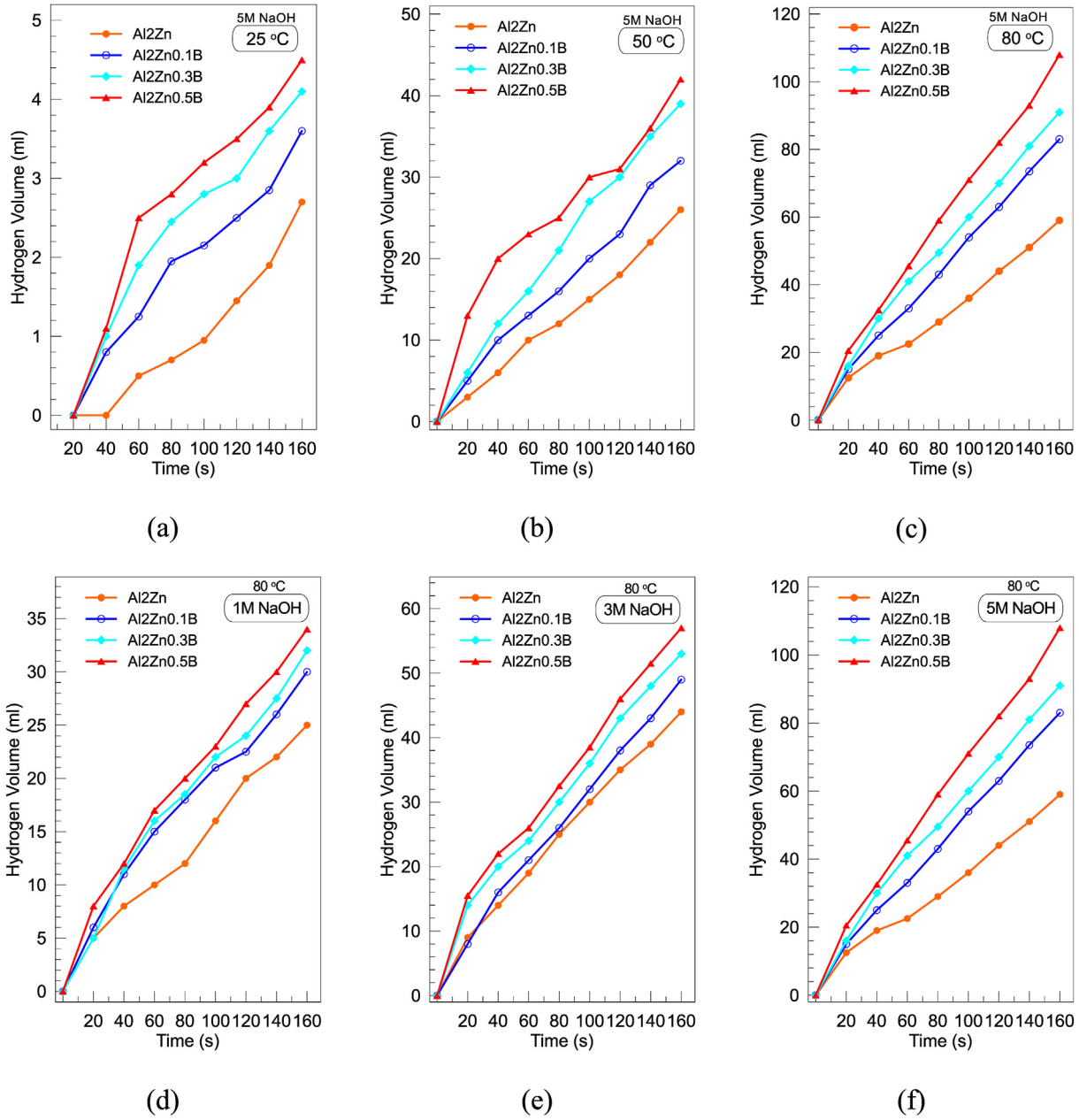

Fig. 2 – Hydrogen generation of alloys' by time a) at 25 °C-5M NaOH, b) at 50 °C-5M NaOH, c) at 80 °C- 5 M NaOH, d) at 80 °C-1M NaOH, e) at 80 °C-3M NaOH and f) at 80 °C-5M NaOH.

Table 1 – Hydrogen gas evaluation rate of alloy samples.

Alloy	Gas evaluation rate (ml min^{-1} cm^{-2})				
	25 °C	50 °C	80 °C		
	5 M NaOH	5 M NaOH	5 M NaOH	3 M NaOH	1 M NaOH
Al2Zn	0.46	4.44	10.07	7.51	4.27
Al2Zn0.1B	0.61	5.46	14.16	8.36	5.12
Al2Zn0.3B	0.70	6.65	15.53	9.04	5.46
Al2Zn0.5B	0.77	7.17	18.43	9.72	5.80

Table 2 – Corrosion rates and activation energies of alloy samples in 5 M NaOH.

Alloy	Corrosion rate (mg cm^{-2} min^{-1})			Activation energy (kJ mol^{-1})
	298 K	323 K	353 K	
Al2Zn	1.88	3.92	10.07	26.717
Al2Zn0.1B	2.39	4.78	11.77	25.372
Al2Zn0.3B	2.73	5.29	12.80	24.575
Al2Zn0.5B	3.07	5.97	13.48	23.526

alloy, hydrogen production amount is increased around 83% by 108 ml in Al2Zn0.5B alloy. By addition of 0.5wt.% addition of B to Al2Zn alloy, G_{H2} value is changed from 10.07 ml min^{-1} cm^{-2} to 18.43 ml min^{-1} cm^{-2} with 1.83 times higher value.

In Fig. 2d, e and f, experiments are performed at 80 °C constant temperature during 160 s by changing alkaline aqueous solution concentration from 1 to 5 M. As seen in Fig. 2d, e and f, increasing the solution concentration, hydrogen production amount is enhanced, significantly. As seen in different concentration experiments, the highest hydrogen production is obtained in Al2Zn0.5B ternary alloy. Increasing the addition of B to Al2Zn alloy increased the hydrogen production value, remarkably. In 1, 3 and 5 M concentration of NaOH aqueous solutions, maximum hydrogen production amounts are measured in Al2Zn0.5B as 34 ml, 57 ml and 108 ml, respectively. Moreover, for 3 M NaOH aqueous solution experiments, while hydrogen production and G_{H2} is measured as 57 ml and 9.72 ml min^{-1} cm^{-2} in Al2Zn0.5B alloy, for 5 M NaOH aqueous solution experiments, Al2Zn alloys hydrogen production and G_{H2} values are measured as 59 ml and 10.07 ml min^{-1} cm^{-2}, respectively. Here it is clear that, for 3 M NaOH in Al2Zn0.5B alloy and 5 M NaOH concentrations with Al2Zn alloy, hydrogen production and G_{H2} values are very similar. Hereby, addition the certain amount of B to Al2Zn alloy, decrease the NaOH concentration to obtain the same amount of hydrogen gas. It is highly crucial in hydrogen generation reactions that arranging proper temperature and solution concentration considering production stability, time and energy consumption [43]. For example, technological devices, such as fuel cells, which can use hydrogen directly to produce electricity. Solution temperature, alkaline concentration and alloying metal contents are highly important parameters for stable energy conversion in these devices. Thus, in this study optimum temperature, concentration and amount of B doping to Al2Zn alloys are investigated.

Kinetic parameters

In Table 2, corrosion rates and activation energies of alloy samples can be seen. At 25 °C, the corrosion rate of Al2Zn0.5B alloy is 3.07 mg cm^{-2} min^{-1} while it is 13.48 mg cm^{-2} min^{-1} at 80 °C. As mentioned previously, addition of B to Al2Zn alloy is increased the hydrogen generation amount. The reason of this improvement may be due to enhanced corrosion value of the samples. In alkaline media, aluminium corrosion reaction can be shown as below [44]:

$$Al + OH^- + 3/4\ O_2 + 3/2\ H_2O \rightarrow Al(OH)_4^- \quad (4)$$

In this reaction, aluminium is consumed, and hydrogen generation reactions are taken place as below:

$$Al + 3/2\ H_2O + OH^- \rightarrow 3/2\ H_2 + Al(OH)_4^- \quad (5)$$

As mentioned before, passive oxide film on the samples may cause slower reactions for hydrogen generation. However, by increasing temperature, this film may become more porous and less protective. For this reason, it is caused higher corrosion ratio. This situation may be explained by high chemical activity due to accumulated OH^- ions and consumed $Al(OH)_4^-$ ions between oxide film and solution interface enhanced chemical solubility [44,45].

Moreover, to investigate the relations of reactions with temperature between alloy samples and solution, reaction kinetic must be clarified. The reaction kinetics can be explained by Arrhenius equation as below [46]:

$$C_r = B \exp\left(-\frac{E_a}{RT}\right) \quad (6)$$

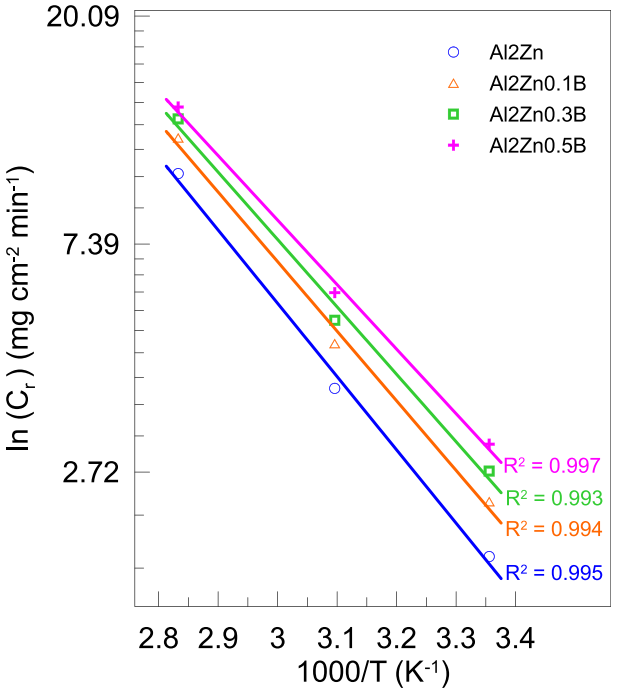

Fig. 3 – Arrhenius plot for the alloys in 5 M NaOH media.

Here, C_r, represents the alloy samples' corrosion ratio in alkaline media, R is universal gas constant (8.314 J mol^{-1} K^{-1}), T is absolute temperature, E_a is activation energy in alkaline media and B represents the pre-exponential factor. The activation energy of binary Al2Zn and ternary Al2Zn-B alloys are calculated via Eq. (6). In Fig. 3, Arrhenius plot (lnC_r vs 1000/T) of different alloys can be seen.

As seen in Fig. 3, B added Al2Zn alloys have the lower activation energy value than Al2Zn alloy sample. Calculated slope of the curves in Fig. 3 is listed as Table 2 to compare E_a values of different samples.

As seen in Table 2, Al2Zn binary alloy has the highest E_a value by 26.717 kJ mol^{-1} while the lowest value is calculated in Al2Zn0.5B ternary alloy as 23.526 kJ mol^{-1}. These results prove that, in 5 M NaOH aqueous solution, addition of B to Al2Zn alloy increase the hydrogen production and corrosion ratio. In Table 3, kinetic parameter comparison from literature studies can be seen.

As seen in Table 3, activation energy values are meaningful compared to literature data. Calculated activation energy values are obtained between 13.25 and 43.814 kJ mol^{-1}. By alloying of Al and different solutions, activation energy can be changed.

Detailed surface analysis of alloys

FE-SEM and FE-SEM-EDX analysis

Samples, which are performed in 5 M NaOH solution for 160 s are characterized after reactions to observe effect of corrosion and oxide films on the surface. Fig. 4 shows the FE-SEM images

Table 3 – Kinetic parameter comparison from literature studies.

Sample	Temperature Range (K)	Solutions and Concentrations	Activation energy (kJ mol^{-1})	Ref.
Al2Zn0.5B	298–353 K	NaOH, 5 M	23.526	This study
Al rod	298–338	Zinc Amalgam, NA	43.4	[47]
Al6063	303–323 K	NaOH, 0.05 M	18.43	[44]
Al6063	303–323 K	NaOH, 0.5 M	13.25	[44]
50wt.% Al-34wt.% Ga-11wt.% In-5wt.% Sn	297–338 K	Water, NA	43.814	[48]
$Ni_{20}Al_{80}$	293–333 K	0.2310–0.6931 M NaOH	42.50	[49]

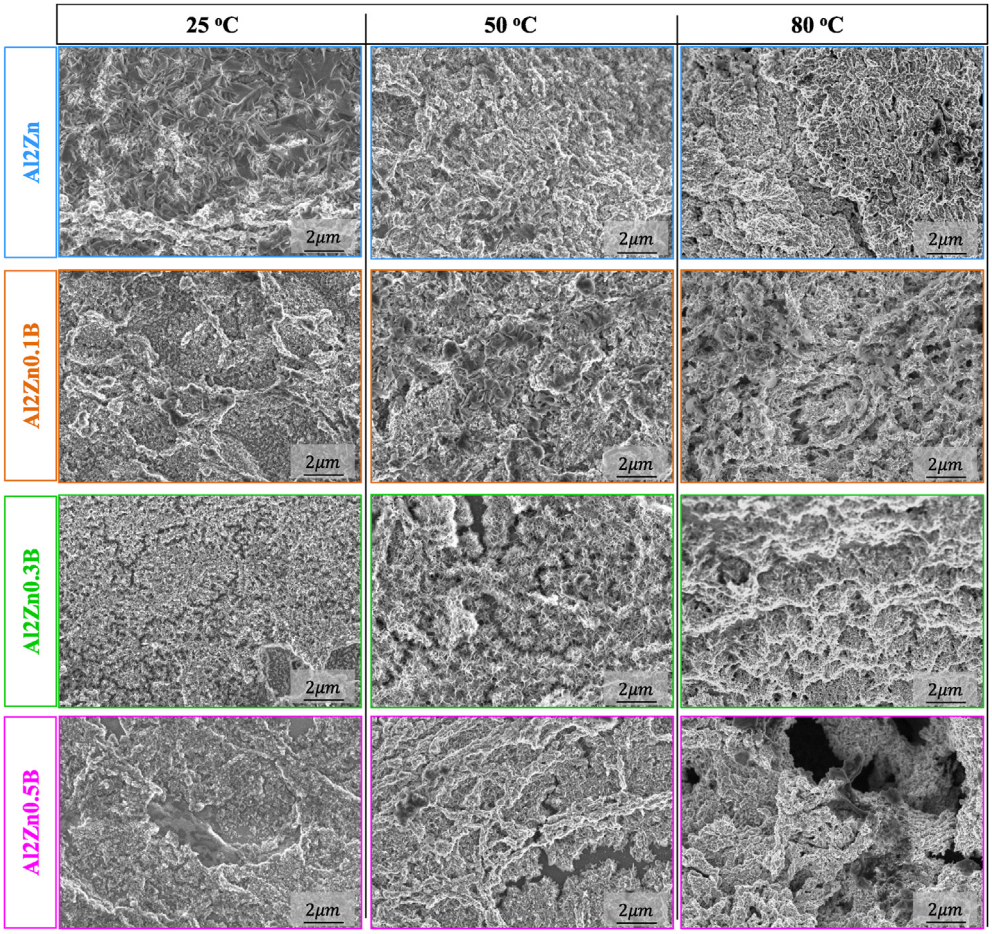

Fig. 4 – FE-SEM imaging of alloys after the corrosion in alkaline media.

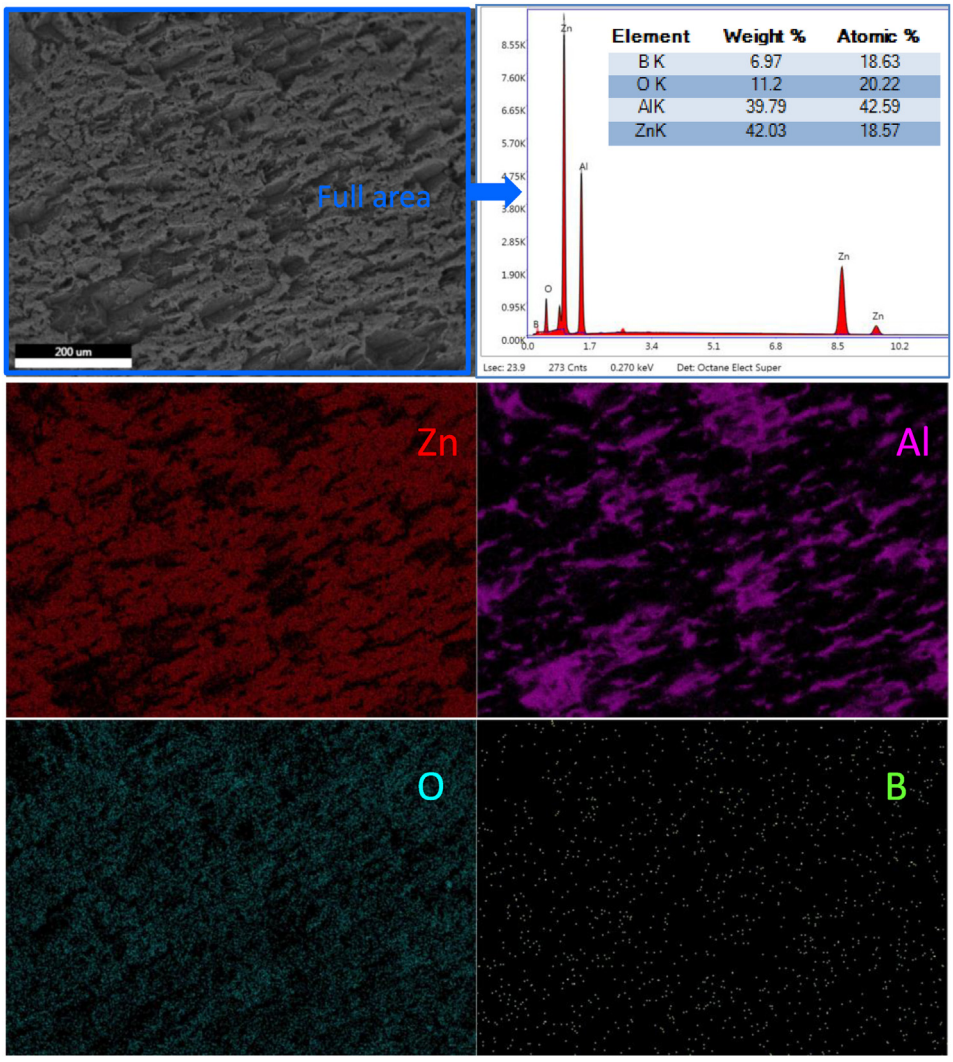

Fig. 5 – FE-SEM image mapping and FE-SEM-EDX analysis of Al2Zn0.5B alloy after the corrosion in alkaline media.

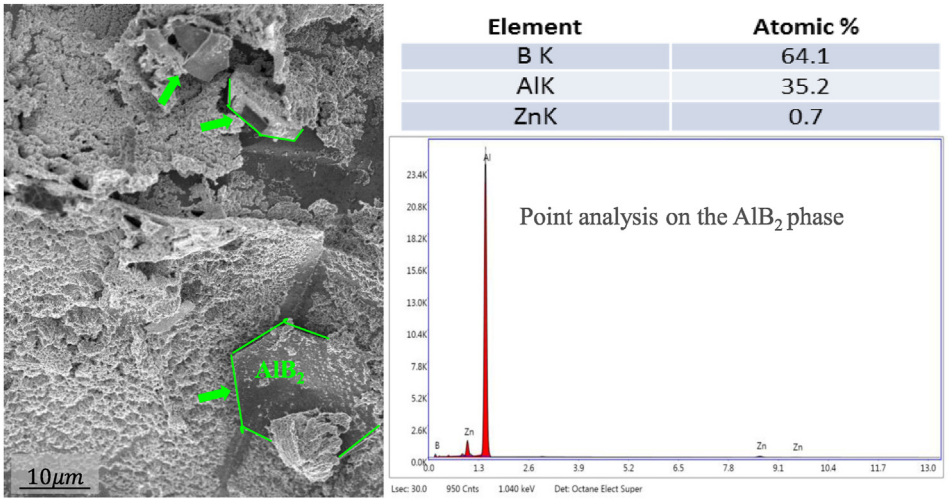

Fig. 6 – Microstructure image of AlB_2 particles and FE-SEM-EDX analysis in Al2Zn0.5B alloy.

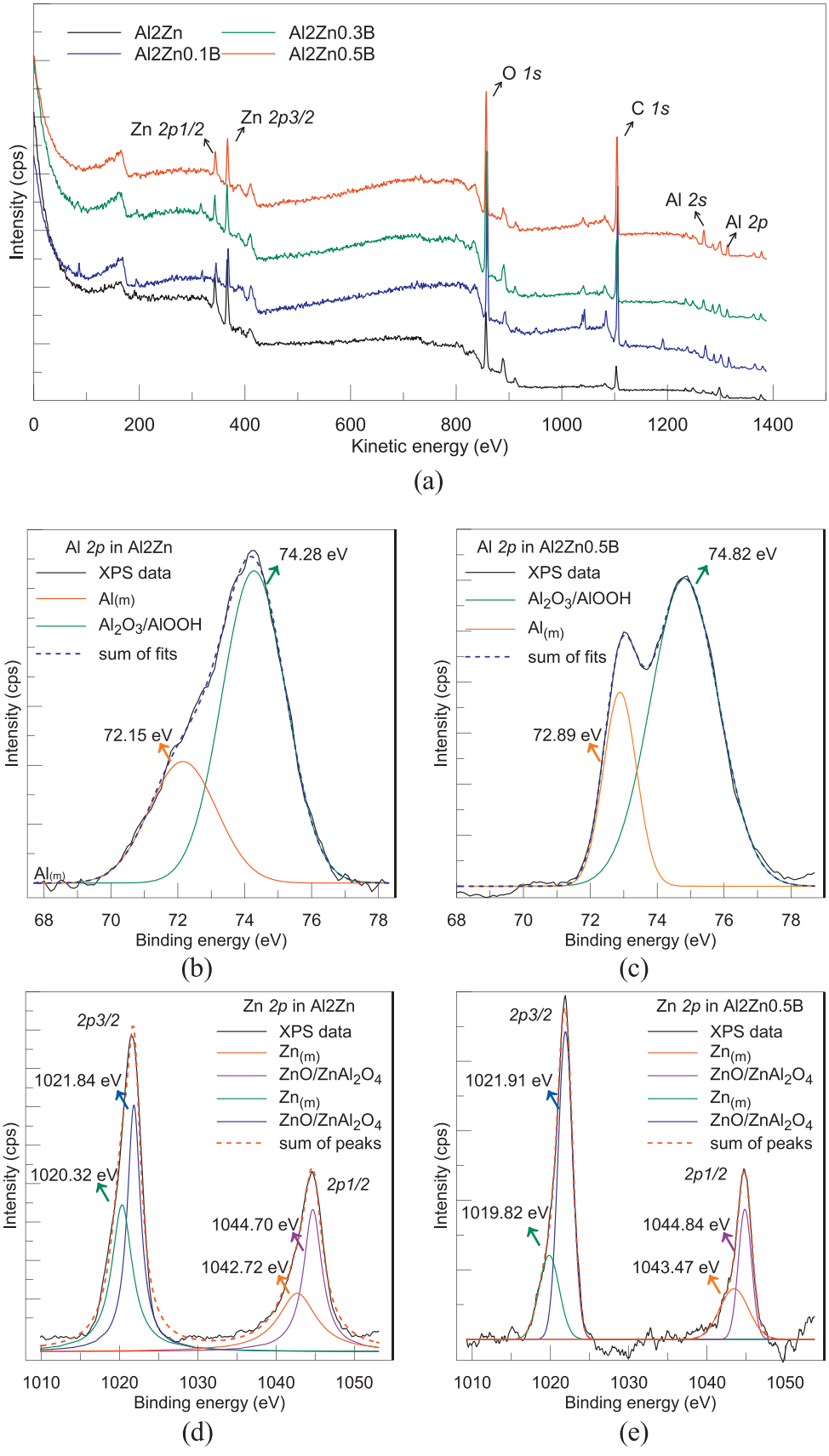

Fig. 7 – a) General XPS spectra acquired on the surface of Al2Zn, Al2Zn0.1B, Al2Zn0.3B and Al2Zn0.5B alloys, high-resolution Al *2p* XPS spectrum acquired on the b) Al2Zn, c) Al2Zn0.5B, High-resolution Zn *2p* XPS spectrum acquired on the d) Al2Zn and e) Al2Zn0.5B alloys.

different temperature and B addition affect can be seen for different alloys.

Increasing alkaline media temperature to the 80 °C, oxide film amount is increased, and more porous structures are observed. For all temperatures, increasing of B addition to the Al2Zn alloy, oxide films are observed as more cracked. This porous and cracked structures support the low activation energy and higher corrosion ratio of B addition to the Al2Zn alloys. Formation of AlB_2 phase particles may cause more cracked and porous structure of oxide film.

In Fig. 5, FE-SEM image mapping and FE-SEM-EDX analysis of Al2Zn0.5B alloy after the corrosion in alkaline media can be seen for a phase region.

As seen in Fig. 5, Al density is very clear around the cracked regions in SEM mapping images. From these regions, Al can be easily contact with alkaline solution to produce higher hydrogen amount. Zn may form a passive oxide films in alkaline media. These Zn oxide compounds formed oxide films on the Al surface, and they are classified as two-types [36]. These oxide films are compact and protective between Al alloy surface and alkaline electrolyte [50]. Thus, Zn oxide compounds are more obvious than Al oxides on the surface. As seen in Fig. 5, in SEM mapping images, in dense Zn regions, there are more intense O elements.

In FE-SEM-EDX analysis of full area, peaks of elements which forms the alloy (Al-Zn-B) and O element can be seen. Zn element forms protective surface film on Al surface as mentioned in the literature [36,51]. In Fig. 6, microstructure image of AlB_2 particles and FE-SEM-EDX analysis in Al2Zn0.5B alloy can be seen.

As seen in Fig. 6, AlB_2 is formed some cracks on the oxide film. It is known that AlB_2 particles are made oxide films more fragile and decreased the corrosion resistance [52]. Moreover, B element has randomized distribution in the structure. As seen in Fig. 5, AlB2 phase is validated by FE-SEM-EDX analysis with their atomic ratio, too.

XPS analysis for alloys

Fig. 7 displays the general XPS spectra and high-resolution Al and Zn *2p* XPS spectrum acquired on the surface of the alloys. From these spectra, it is concluded that, zinc rich surfaces are formed, and a significant amount of oxide was observed. In addition, some aluminum peaks are observed due to the porous structure formed due to boron doping observed in SEM images. Also, an amount of carbon contamination is observed.

Fig. 7b and c shows the evolution of the spectra of the A1 *2p* core level in Al2Zn and Al2Zn0.5B alloys. The binding energy (BE) values of an electron depends on several factors. Such as photoemission energy, formal oxidation states of atoms and local chemical and physical environment. This local oxidation states and environmental factors can be caused a small shift in the peak positions in the spectrum. Such shifts are called as a chemical shift and easily observable and interpretable in XPS spectra [53]. The A1 *2p* line always exhibits a double structure attributed to metallic (low BE ~72 eV) and oxidized states of aluminum (~74 eV) [54]. When the spectrum is deconvoluted, binding energies are obtained as 72.15 eV and 74.28 eV for Al2Zn, 72.89 eV and 74.82 eV for Al2Zn0.5B, respectively. This shift in binding energies is directly related to boron addition and oxidation states of aluminum [54]. In addition, the etching process carried out in an alkaline environment which influences this chemical shift. It is clear here that, because of B addition, the alloy has a more porous structure and it has a significant effect on the oxidation process.

Fig. 7 d and e show the evolution of the spectra of the Zn *2p* core level in Al2Zn and Al2Zn0.5B alloys. Both spectra have two peaks and these peaks belongs to the *2p1/2* and *2p3/2* orbitals of the zinc atom. When the peaks are deconvoluted, it is seen that both the presence of the metallic phase and the oxidized phase for Zn *2p3/2*, similar to Al. The binding energy for ZnO is 1021.84 eV for the *2p3/2* orbital, and this binding energy value is also indicated that formation of $ZnAl_2O_4$ [55–57]. The presence of Zn at the surface as an alloying element promotes the nucleation of $ZnAl_2O_4$ spinel and gives rise to increased defects and cracking of the thin surface layer [56]. According to the Al Shayeb et al. [57] the incorporation of Sn into the bulk of the alloy is more easier than its incorporation into the Al surface. So similar behavior observed in our B added Al-Zn alloy as stated in SEM analysis. Both Zn *2p1/2* and *2p3/2* peaks indicate the existence of the oxide phase and shifted to the higher in binding energies. Also, binding energy difference with the Zn *2p1/2* and *2p3/2* is close to 23 eV for both alloys and consistent with the literature [54].

Conclusions

In presented work, B additions to Al2Zn alloys are investigated by changing the B addition amount, NaOH concentration and temperature. Considering the hydrogen generation and G_{H2} values, the highest performance is obtained at 80 °C temperature, 5 M NaOH concentration and 5wt.%B addition. In Al2Zn0.5B alloy, 18.43 ml min^{-1} cm^{-2} G_{H2} value and 13.48 mg min^{-1} cm^{-2} corrosion rate is obtained. By the help of convenient alloying to Al, hydrogen generation behaviour can be developed, remarkably. For example, Zn improves the hydrogen production amount of Al alloys. Furthermore, in this study, 83% extra improvement is obtained by 5wt.%B addition to the Al2Zn alloy. Temperature affect the kinetic parameters of Al hydrogen production reactions. Temperature range, which is investigated in experimental studies, by addition of B to Al2Zn alloy, activation energy values are diminished from 26.717 to 23.526 kJ mol^{-1}. According to surface oxide film examinations, Al and Zn elements oxide form is formed and this oxide films are more fragile and porous by the help of AlB_2 phase. In our future studies, intermetallic particles which are located grain boundaries of the aluminium alloys and ternary alloys with randomly located B contained structures' hydrogen production performance will be studied. Then, effect of higher B doping to the different Al alloys in several temperature and concentration conditions will be investigated.

Declaration of competing interest

The authors declare that they have no known competing financial interests or personal relationships that could have appeared to influence the work reported in this paper.

Acknowledgements

The authors would like to thank the Scientific Research Projects Unit of Erciyes University for funding and supporting the project under the contract numbers FKB-2020-9703 and FKB-2019-9134.

REFERENCES

[1] Wang H, Chang Y, Dong S, Lei Z, Zhu Q, Luo P, et al. Investigation on hydrogen production using multicomponent aluminum alloys at mild conditions and its mechanism. Int J Hydrogen Energy 2013;38:1236–43.
[2] Wang H, Leung DY, Leung M, Ni M. A review on hydrogen production using aluminum and aluminum alloys. Renew Sustain Energy Rev 2009;13:845–53.
[3] Kotay SM, Das D. Biohydrogen as a renewable energy resource—prospects and potentials. Int J Hydrogen Energy 2008;33:258–63.
[4] Walter MG, Warren EL, McKone JR, Boettcher SW, Mi Q, Santori EA, et al. Solar water splitting cells. Chem Rev 2010;110:6446–73.
[5] Kaya MF, Demir N, Rees NV, El-Kharouf A. Improving PEM water electrolyser's performance by magnetic field application. Appl Energy 2020;264:114721.
[6] Ni M, Leung MK, Leung DY, Sumathy K. A review and recent developments in photocatalytic water-splitting using TiO2 for hydrogen production. Renew Sustain Energy Rev 2007;11:401–25.
[7] Lutz AE, Bradshaw RW, Bromberg L, Rabinovich A. Thermodynamic analysis of hydrogen production by partial oxidation reforming. Int J Hydrogen Energy 2004;29:809–16.
[8] Milne TA, Elam CC, Evans RJ. Hydrogen from biomass: state of the art and research challenges. Golden, CO (US): National Renewable Energy Lab.; 2002.
[9] Kravchenko O, Semenenko K, Bulychev B, Kalmykov K. Activation of aluminum metal and its reaction with water. J Alloys Compd 2005;397:58–62.
[10] Yang S, Knickle H. Design and analysis of aluminum/air battery system for electric vehicles. J Power Sources 2002;112:162–73.
[11] Vargel C. Corrosion of aluminium. Elsevier; 2020.
[12] Schlapbach L, Züttel A. Hydrogen-storage materials for mobile applications. In: Materials for sustainable energy: a collection of peer-reviewed research and review articles from nature publishing group. World Scientific; 2011. p. 265–70.
[13] Ho C-Y, Huang C-H. Enhancement of hydrogen generation using waste aluminum cans hydrolysis in low alkaline deionized water. Int J Hydrogen Energy 2016;41:3741–7.
[14] Huang T, Gao Q, Liu D, Xu S, Guo C, Zou J, et al. Preparation of Al-Ga-In-Sn-Bi quinary alloy and its hydrogen production via water splitting. Int J Hydrogen Energy 2015;40:2354–62.
[15] Czech E, Troczynski T. Hydrogen generation through massive corrosion of deformed aluminum in water. Int J Hydrogen Energy 2010;35:1029–37.
[16] Aleksandrov YA, Tsyganova E, Pisarev A. Reaction of aluminum with dilute aqueous NaOH solutions. Russ J Gen Chem 2003;73.
[17] Rosenband V, Gany A. Application of activated aluminum powder for generation of hydrogen from water. Int J Hydrogen Energy 2010;35:10898–904.
[18] Liu S, Fan M-q, Wang C, Huang Y-x, Chen D, Bai L-q, et al. Hydrogen generation by hydrolysis of Al–Li–Bi–NaCl mixture with pure water. Int J Hydrogen Energy 2012;37:1014–20.
[19] Wang C, Yang T, Liu Y, Ruan J, Yang S, Liu X. Hydrogen generation by the hydrolysis of magnesiumealuminumeiron material in aqueous solutions. Int J Hydrogen Energy 2014;39:e10852.
[20] Brindley GF. Composition of matter for generating hydrogen. Google Patents; 1909.
[21] Brindley GF, Bennie PM. Composition of matter for manufacturing hydrogen gas. Google Patents; 1909.
[22] Gill GC. Hydrogen generator. Google Patents; 1955.
[23] Checketts JH. Hydrogen generation pelletized fuel. Google Patents; 1998.
[24] Andersen ER, Andersen EJ. Method for producing hydrogen. Google Patents; 2003.
[25] Andersen EJ. Renewable energy carrier system and method. Google Patents; 2006.
[26] Hiraki T, Yamauchi S, Iida M, Uesugi H, Akiyama T. Process for recycling waste aluminum with generation of high-pressure hydrogen. Environ Sci Technol 2007;41:4454–7.
[27] Dupiano P, Stamatis D, Dreizin EL. Hydrogen production by reacting water with mechanically milled composite aluminum-metal oxide powders. Int J Hydrogen Energy 2011;36:4781–91.
[28] Chen X, Zhao Z, Hao M, Wang D. Hydrogen generation by splitting water with Al–Li alloys. Int J Energy Res 2013;37:1624–34.
[29] Luo H, Liu J, Pu X, Liang J, Wang Z, Wang F, et al. Hydrogen generation from highly activated Al–Ce composite materials in pure water. J Am Ceram Soc 2011;94:3976–82.
[30] Zhao Z, Chen X, Hao M. Hydrogen generation by splitting water with Al–Ca alloy. Energy 2011;36:2782–7.
[31] Fan M-Q, Xu F, Sun L-X. Studies on hydrogen generation characteristics of hydrolysis of the ball milling Al-based materials in pure water. Int J Hydrogen Energy 2007;32:2809–15.
[32] Ilyukhina A, Ilyukhin A, Shkolnikov E. Hydrogen generation from water by means of activated aluminum. Int J Hydrogen Energy 2012;37:16382–7.
[33] Wang W, Chen D, Yang K. Investigation on microstructure and hydrogen generation performance of Al-rich alloys. Int J Hydrogen Energy 2010;35:12011–9.
[34] Du Preez S, Bessarabov D. Hydrogen generation by the hydrolysis of mechanochemically activated aluminum-tin-indium composites in pure water. Int J Hydrogen Energy 2018;43:21398–413.
[35] Du B, He T, Liu G, Chen W, Wang Y, Wang W, et al. Al-water reactivity of AlMgGaInSn alloys used for hydraulic fracturing tools. Int J Hydrogen Energy 2018;43:7201–15.
[36] Park I-J, Choi S-R, Kim J-G. Aluminum anode for aluminum-air battery–Part II: influence of in addition on the electrochemical characteristics of Al-Zn alloy in alkaline solution. J Power Sources 2017;357:47–55.
[37] Zhang F, Edalati K, Arita M, Horita Z. Hydrolytic hydrogen production on Al–Sn–Zn alloys processed by high-pressure torsion. Materials 2018;11:1209.
[38] Zhang P, Liu X, Xue J, Jiang K. The role of microstructural evolution in improving energy conversion of Al-based anodes for metal-air batteries. J Power Sources 2020;451:227806.
[39] Liu X, Zhang P, Xue J. The role of micro-naoscale AlSb precipitates in improving the discharge performance of Al-Sb alloy anodes for Al-air batteries. J Power Sources 2019;425:186–94.
[40] Ma J, Wen J, Ren F, Wang G, Xiong Y. Electrochemical performance of Al– Mg– Sn based alloys as anode for Al-air battery. J Electrochem Soc 2016;163:A1759.
[41] Gao X, Xue J, Liu X, Shi G. Effects of heat treatment on the electrochemical performance of Al based anode materials for

air-battery. In: TMS Annual Meeting & Exhibition. Springer; 2018. p. 99–108.
[42] Ma J, Wen J, Gao J, Li Q. Performance of Al–0.5 Mg–0.02 Ga–0.1 Sn–0.5 Mn as anode for Al–air battery in NaCl solutions. J Power Sources 2014;253:419–23.
[43] Xu S, Cui Y, Yang L, Liu J. Instant hydrogen production using Ga-In-Sn-Bi alloy-activated Al-water reaction for hydrogen fuel cells. J Renew Sustain Energy 2020;12:014701.
[44] Deepa P, Padmalatha R. Corrosion behaviour of 6063 aluminium alloy in acidic and in alkaline media. Arabian J chem 2017;10:S2234–44.
[45] Foley R, Nguyen T. The chemical nature of aluminum corrosion: V. Energy transfer in aluminum dissolution. J Electrochem Soc 1982;129:464.
[46] Szauer T, Brandt A. Adsorption of oleates of various amines on iron in acidic solution. Electrochim Acta 1981;26:1253–6.
[47] Huang X-n, Lv C-j, Huang Y-x, Liu S, Wang C, Chen D. Effects of amalgam on hydrogen generation by hydrolysis of aluminum with water. Int J Hydrogen Energy 2011;36:15119–24.
[48] Ziebarth JT, Woodall JM, Kramer RA, Choi G. Liquid phase-enabled reaction of Al–Ga and Al–Ga–In–Sn alloys with water. Int J Hydrogen Energy 2011;36:5271–9.
[49] Hu H, Qiao M, Pei Y, Fan K, Li H, Zong B, et al. Kinetics of hydrogen evolution in alkali leaching of rapidly quenched Ni–Al alloy. Appl Catal Gen 2003;252:173–83.
[50] Tang Y, Lu L, Roesky HW, Wang L, Huang B. The effect of zinc on the aluminum anode of the aluminum–air battery. J Power Sources 2004;138:313–8.
[51] Lee H, Listyawan TA, Park N, Kim G, Chang I. Effect of Zn addition on electrochemical performance of Al–air battery. Int J Precision Eng Manufact Green Technol 2020;7:505–9.
[52] Elcicek H, Savaş Ö, Aydin Z, Özdemir O, Kayikci R. Corrosion behavior of in-situ AlB2/Al-Cu metal matrix composite. Acta Phys Pol, A 2016;129.
[53] Verma HR. Atomic and nuclear analytical methods. Berlin: Springer; 2007.
[54] Moulder JF, Chastain J, King RC. Handbook of x-ray photoelectron spectroscopy: A reference book of standard spectra for identification and interpretation of Xps data. Minnesota USA: Perkin-Elmer Corporatioon, Physical Electronics Division; 1995.
[55] Strohmeier BR. Zinc aluminate (ZnAl2O4) by XPS. Surf Sci Spectra 1994;3:128–34.
[56] Breslin CB, Friery LP, Carroll WM. The electrochemical behaviour of Al·Zn·In and Al·Zn·Hg alloys in aqueous halide solutions. Corrosion Sci 1994;36:85–97.
[57] El Shayeb H, Abd El Wahab F, El Abedin SZ. Electrochemical behaviour of Al, Al–Sn, Al–Zn and Al–Zn–Sn alloys in chloride solutions containing stannous ions. Corrosion Sci 2001;43:655–69.